In-beam γ-ray spectroscopy of ^{40}Cl

D. P. Balamuth, U. J. Hüttmeier,* and J. W. Arrison
Department of Physics, University of Pennsylvania, Philadelphia, Pennsylvania 19104
(Received 23 August 1993)

The structure of the neutron-rich ($T_z = 3$) nucleus ^{40}Cl is investigated by measuring α-p-γ-γ and α-p-n-γ-γ coincidences using the heavy-ion fusion-evaporation reaction ^{9}Be(^{36}S,αp)^{40}Cl. A total of 18 in-beam transitions in ^{40}Cl are identified and a level scheme is constructed up to spin (8^-) and 4.087 MeV excitation energy. The experimental results are discussed in the context of previous work and compared to shell-model predictions. Excitation energies of the negative parity yrast states and relative electromagnetic transition strengths obtained from calculations based on the full $(2s, 1d)^{21}(1f2p)^3$ configuration space are in good agreement with the experimental results.

PACS number(s): 23.20.−g, 27.40.+z

I. INTRODUCTION

The recent development of efficient charged-particle-γ coincidence techniques has made new regions of nuclei far from stability accessible to experimental investigation. These nuclei can provide an excellent test of theoretical models of nuclear structure. In particular, neutron-rich nuclei in the $A \approx 40$ mass region can be used to test shell-model predictions employing effective Hamiltonians derived from systematic fits to the properties of nuclei near stability. For the systems of interest, the lowest-energy proton orbits are in the $1s$-$0d$ shell, whereas the neutrons are filling orbits in the $0f$-$1p$ shell. The shell-model calculations of interest thus require matrix elements both within each major shell as well as cross shell.

The nucleus ^{40}Cl has recently received considerable attention, both from theorists and experimentalists. On the experimental side, the investigation of neutron-rich nuclei far from stability is made difficult by their relative inaccessibility. Although the cross sections are small, charged-particle-induced transfer reactions have successfully been used to provide information on excited levels of nuclei far from stability. Using the charge exchange reaction ^{40}Ar(^{7}Li,^{7}Be)^{40}Cl, excited states in ^{40}Cl were first reported by Fifield *et al.* [1]. Dufour *et al.* [2] reported the first electromagnetic transitions in ^{40}Cl in a study of the β^- decay of ^{40}S by produced via projectile fragmentation and subsequent isotopic separation. Recently, the first observation of in-beam electromagnetic decays was reported by Kozub *et al.* [3], using the heavy-ion reaction ^{9}Be(^{36}S,αp)^{40}Cl. This experiment was carried out at Argonne National Laboratory using eight Compton-suppressed Ge detectors in combination with two solid state detector telescopes subtending a small solid angle ($\approx 2.2\%$ of 4π).

Shell-model calculations for ^{40}Cl have been reported by Woods [4], by Ji and Wildenthal [5], and by Warburton and Becker [6]. The first predictions of excitation energies of negative parity states in ^{40}Cl by Woods were based on a $(\pi s_{1/2}, d_{3/2})^9$, $(\nu f_{7/2}, p_{3/2})^3$ configuration space. In the Ji-Wildenthal calculations only neutron and proton $d_{3/2}$, $f_{7/2}$ orbitals were considered, but particle-hole excitations between the two oscillator shells were allowed. The most recent calculations by Warburton and Becker are based on the full $(2s, 1d)^{21}(1f2p)^3$ model space but, similar to Woods, did not include multiparticle-multihole excitations. In addition to excitation energies, Ref. [6] also gives predictions of electromagnetic transition strengths that can provide a sensitive test of the model when compared to experiment. All calculations correctly predict $J^\pi = 2^-$ for the ground state of ^{40}Cl, and agree that the first excited state should have $J^\pi = 1^-$ at an excitation energy anywhere from 64 to 253 keV. The predictions for excited states in general, however, vary considerably and illustrate the need for additional experimental information.

In the present work we have investigated the structure of ^{40}Cl by measuring up to fivefold coincidences ($\alpha pn\gamma\gamma$) using the reaction ^{9}Be(^{36}S,αp)^{40}Cl. Our experiment differs from previous work in several important respects. First, charged particles were detected with the University of Pennsylvania 4π charged-particle array [7]. The good granularity and large solid angle coverage of this device (up to 19 particle telescopes were used in the present experiments covering approximately 72% of 4π) resulted in an efficiency for the detection of two charged particles (one α particle and one proton) more than two orders of magnitude higher than that obtained in Ref. [3]. This improvement provides good statistics for γ-γ coincidences gated on a specific combination of charged particles and reveals the data of interest in considerably more spectroscopic detail than had been done previously. A second improvement over previous work is the measurement of neutrons in coincidence with $\alpha p\gamma$ events. This permits the distinction between αp and αpn evaporation to be made in a way which does not depend on the results of model calculations of the evaporation process.

The paper is organized as follows. Experimental de-

*Present address: Seeliger & Partner, Otto-Beck-Str. 32-34, D-68165 Mannheim, Germany.

tails are given in the following section. The next two sections deal with the identification of transitions in ^{40}Cl from the particle-γ coincidence measurements and the construction of a level scheme from the particle-γ-γ data. Our goal has been to achieve sufficient sensitivity to extend the yrast level structure to higher spins and also to detect relatively weak transitions between the yrast states which are predicted by the shell model. Some new information on nonyrast states has also been obtained. We conclude with a summary and discussion of the experimental results in the context of theoretical predictions.

II. EXPERIMENTAL PROCEDURE

Until considerable improvements are made in the development of radioactive secondary beams, the use of heavy-ion fusion-evaporation reactions with stable targets and projectiles is the most efficient experimental technique available at present to study states up to high spin in very neutron-rich midmass nuclei. A compound nucleus so formed in this mass region decays predominantly by multiple neutron evaporation towards residual systems closer to stability. The most neutron-rich nuclei, however, can be produced by pure multiple charged-particle evaporation channels with very small cross sections, generally in the range of sub-μb to a few mb. In a γ-singles or γ-γ coincidence spectrum, the transitions of interest are thus obscured by the Compton background from the dominating xn, pxn, and αxn evaporation channels, produced with cross sections of hundreds of mb.

An additional experimental complication in the present reaction results from the fact that ^{8}Be is unstable against decay into two α particles. Direct transfer of the last loosely bound neutron in ^{9}Be to the ^{36}S projectile via a direct reaction, which has a total cross section comparable to the strongest channels populated in fusion-evaporation reactions, not only adds to the general γ-ray background, but is also not eliminated by a trigger which requires the detection of two charged particles. This emphasizes the importance of good particle identification in experiments of this type. (Note that discrimination against the direct reaction background is also aided by the relatively lower γ-ray multiplicity associated with these processes.)

All experiments were conducted with a beam extracted from a cathode of isotopically enriched ^{34}S which, as a by-product of the enrichment process, contained about 1.0% ^{36}S. Beam currents as high as 1 particle μA of ^{36}S were obtained from our sputter source [8] during a test run with an ionization efficiency of approximately 3%. The experiments were performed with beam currents of up to 500 nA injected into the University of Pennsylvania FN tandem Van de Graaff accelerator operating at terminal potentials up to 10.5 MV. Beam energies of 100 and 105 MeV were chosen for the present experiments based on the excitation function for production of ^{40}Cl predicted by the evaporation model codes CASCADE [9] and PACE2 [10].

In the present work ^{40}Cl is produced with a cross section of 2.0 ± 0.5 mb in the reaction ^{9}Be(^{36}S,αp)^{40}Cl measured at a beam energy of 105 MeV. The cross section is inferred from the efficiency-corrected intensity of the strongest transition of ^{40}Cl in the γ-ray singles spectrum, taking into account the relative intensity of two other transitions feeding the ground state. The result is checked against the value obtained from the particle-gated γ-ray spectrum corrected for the respective particle detection efficiencies. This corresponds to approximately 0.2% of the total fusion cross section and, taking into account the strong contribution from direct reactions, an even smaller fraction of the total cross section. The experimental difficulties resulting from the small cross section can be seen in the spectrum shown in Fig. 1(a), which shows a portion of the prescaled γ-ray singles spectrum obtained with a Compton-suppressed Ge detector positioned at 135° with respect to the incident beam. The strongest transition in ^{40}Cl at 244 keV is very weak, with an intensity over two orders of magnitude smaller than the strongest transitions, which come from the $3n$ (^{42}Ca) and $p2n$ (^{42}K) channels, and is incompletely resolved from neighboring peaks in the singles spectrum. (Note that ^{40}Cl is a favorable case since most of the decay proceeds via the 244 keV transition to the ground state. The situation would be worse for a more fragmented decay scheme.) Thus a sensitive experimental trigger is required to enhance the signals of interest over the intense background from predominantly neutron channels.

Since the residual system is populated in the present reaction by pure charged-particle evaporation, an efficient multiple charged-particle detector is the experimental trigger of choice. All experiments performed in the course of this investigation involve the detection of γ rays in coincidence with charged particles using the Penn 4π

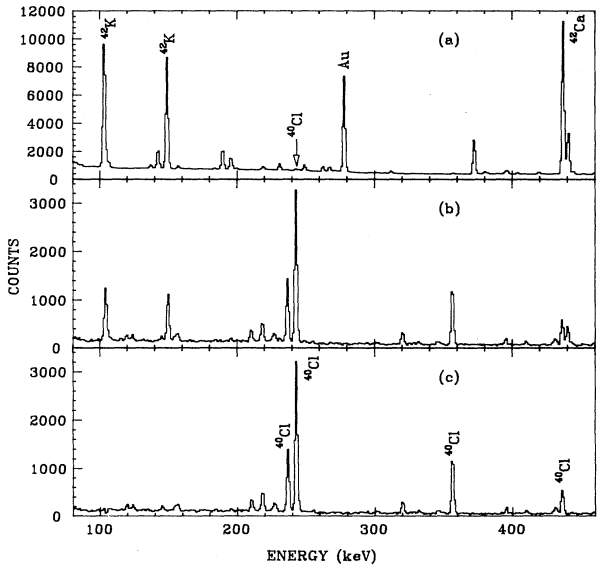

FIG. 1. (a) Prescaled γ-ray singles spectrum. (b) The spectrum in coincidence with one α particle and one proton. (c) Same as (b) with an additional 2 ns particle-particle timing condition.

charged-particle array [7]. The system consists of up to 24 particle detectors of the phoswich scintillator type covering almost 90% of 4π. Because of the strong kinematic focusing of the evaporated particles in the present inverse reaction, the rates in the back angle particle detectors were negligible and thus mainly the forward hemisphere was covered with phoswich telescopes. Most of the back angle and two 90° elements were removed in order to position the Ge detectors close to the target.

The strong production of channels involving a single charged particle in addition to neutrons [e.g., the strong γ rays from the $p2n$ channel ^{42}K seen in Fig. 1(a)] demonstrates the importance of a multiple charged-particle trigger. We required a fourfold coincidence; at least two charged particles and two γ rays were recorded for each event. Note that in Ref. [3] only a threefold coincidence was required. We are able to get reasonable statistical precision with the additional constraint because of the very large detection efficiency of the charged-particle array. The total efficiency for detecting and identifying one α particle and one proton simultaneously in the present setup is about 8%, approximately two orders of magnitude higher than was available in the previous work [3].

Multiple-charged-particle-neutron-γ-γ coincidences were detected using the 4π detector in coincidence with up to six high-resolution Ge detectors, all with an efficiency of approximately 25% [with respect to a 7.6 cm × 7.6 cm NaI(Tl) detector at 1332 keV]. Three of the detectors were equipped with BGO Compton suppression shields and positioned in the horizontal plane at $(\theta,\phi) = (90°,0°)$, $(135°,0°)$, and $(135°,180°)$ with respect to the beam. Here (θ,ϕ) represent polar and azimuthal angles in a spherical coordinate system with the z axis parallel to the beam direction and the y axis vertically downward. The remaining three Ge detectors were unsuppressed and positioned at $(\theta,\phi) = (135°,90°)$, $(110°,45°)$, and $(90°,135°)$. The unsuppressed detectors were equipped with rectangular Pb collimators to reduce Doppler broadening and to match the detection efficiency of the suppressed detectors. The target was a film of Be metal of thickness 500–750 μg/cm^2 evaporated onto a 32 mg/cm^2 Au backing which stopped the incident beam. Neutrons were detected in a large-volume liquid scintillation detector positioned at 0° with respect to the beam. The 45 cm distance of the front face of the neutron detector to the target was sufficient to achieve adequate neutron-γ separation by time of flight relative to the charged-particle detector (for details see Ref. [11]).

Additional charged-particle-γ two-point angular distribution data were obtained in a separate experiment with two Compton-suppressed Ge detectors positioned in the horizontal plane at 90° and 135° with respect to the beam. The relative efficiency of the two Ge detectors required for this comparison was obtained as a function of the γ-ray energy by measurements made in the experimental geometry with radioactive sources placed in the target position. In addition, strong γ rays in ^{42}Ca, the $3n$ evaporation product whose angular distributions are known from previous work using a heavy-ion reaction [12], were used to check the calibration procedure. For these angular distribution measurements, the target was a self-supporting rolled foil of Be metal of thickness 7.8 mg/cm^2, sufficient to stop the incident beam. Because of the thick target and the relatively low dE/dx of Be, the Doppler-broadened line shapes observed at $\theta_\gamma = 135°$ introduced sufficient uncertainty that it was not possible to obtain meaningful angular distributions for transitions from levels with lifetimes comparable to the stopping time. In these cases, the number of counts at 90° was used to estimate the relative intensity. Note that because a thick target was used, the recoil velocity is not well defined and a quantitative evaluation of the observed line shape(s) cannot be related even to an apparent lifetime without making model-dependent assumptions about the energy dependence of the production cross section. However, for a few levels it was clear that the data taken with the thick Be target showed a substantial Doppler-broadened component whereas the corresponding data from the Au-backed target showed mainly a stopped peak at 135°. In these cases, it was possible to place rough limits on the apparent lifetimes which were helpful in suggesting spins and multipolarities (see below).

Data acquisition was performed using a parallel processing system consisting of six MC68000 microprocessors [13]. The data-aquisition software provided the means for complete on-line sorting of all events including a particle-gated $2K \times 2K$ two-dimensional γ-γ coincidence matrix [14]. A hardware trigger was set up to reject γ-γ events in concidence with fewer than two charged particles. A total of 50×10^6 coincidence events with at least two γ rays, two charged particles, and possibly a neutron were recorded on WORM (write once read many) optical disks for subsequent off-line analysis.

III. RESULTS AND ANALYSIS

A. Identification of γ rays in ^{40}Cl

In-beam γ rays previously observed in a heavy-ion reaction using a ^{9}Be target and a ^{36}S beam with an energy of 100 MeV were assigned to ^{40}Cl by Kozub *et al.* [3] on the basis of charged-particle-γ coincidences. With the given target-projectile combination ^{40}Cl was produced by evaporation of one α particle and one proton. The αp-gated spectrum was used to identify the Z of the residual system. Based on fusion-evaporation calculations, which predict a weak cross section for the αpn channel ^{39}Cl at the given bombarding energy, the strongest lines in this αp spectrum were attributed to ^{40}Cl. Transitions in ^{39}Cl, known [15] from studies of the transfer reactions ^{37}Cl(t,p) and ^{40}Ar$(d,^3$He), were weak in the αp-gated spectrum. No γ rays in ^{39}Cl had previously been observed in a heavy-ion reaction.

In the present work we used the same reaction but, in addition to a very-high-efficiency particle spectrometer, our setup included a neutron detector. In order to confirm the previous identification of the residual system, γ-ray spectra were gated on α particles, protons, and neutrons. Figure 1(b) shows the γ-ray spectrum (obtained with the same Ge detector as the singles spec-

trum in the γ-γ coincidence experiment with six Ge detectors) in coincidence with one α particle and one proton (with particle-γ random events subtracted). The striking enhancement of transitions in ^{40}Cl, the αp channel, becomes evident by comparison of this spectrum with the above singles spectrum. The strong transitions of ^{42}K, the $p2n$ channel, are now suppressed by a factor of 175 compared to the corresponding singles spectrum, normalized to the 244 keV transition in ^{40}Cl. However, some feedthrough of γ rays from the strongest reaction channels, in particular ^{42}K, is still present in the αp-gated γ-ray spectrum. This is clearly undesirable, since feedthrough of the strong xn, pxn, and αxn channels in the multiple charged-particle gated γ-ray spectra complicates the identification of previously unobserved γ rays. In addition, Compton scattered γ rays from feedthrough channels will contribute significantly to the background in the particle-gated γ-γ coincidence matrix and will thus adversely affect our sensitivity to weak transitions.

Nearly all of the feedthrough of unwanted channels with one charged particle into the spectrum shown in Fig. 1(b) can be attributed to accidental particle-particle coincidences. An example would be an $\alpha p\gamma\gamma$ event in which the proton and two γ rays result from the production and decay of excited states in ^{42}K, while the α particle comes from an unrelated event. In Fig. 1(b) the effective coincidence resolving time for the charged particles is determined by the electronics as $\tau \approx 20$ ns. The use of fast plastic scintillators for the ΔE measurement in the phoswich detector makes it possible to improve the rejection of accidentals by employing an individual TDC channel for each phoswich. (The TDC channels in such a setup are started by the logical OR of all the particle detectors.) Because leading edge discriminators are used for the 4π phoswich CAMAC modules, optimum timing for the particles requires a correction (made in software) for walk as a function of pulse height. With such a correction the full width at half maximum (FWHM) of the timing observed between two elements of the array was approximately 1.1 ns.

Requiring the improved particle-particle timing constraint as an additional condition on the particle-gated γ-ray spectra yields the spectrum shown in Fig. 1c. The improvement in the peak-to-background ratio for the 244 keV transition in ^{40}Cl in this spectrum compared to the singles spectrum shown in Fig. 1(a) is approximately 500. Feedthrough from transitions in ^{42}K (the strongest transitions have energies of 107, 150, and 441 keV) is no longer visible.

The present data also provide clear discrimination between γ rays resulting from transitions in the αp and αpn reaction products. This is illustrated in Fig. 2, where a portion of the αpn-gated spectrum of γ rays is compared to the corresponding spectrum without the neutron gate. (In Fig. 2 the spectra of all six Ge detectors have been combined to improve the statistics; the small contribution of γ-ray feedthrough into the neutron-gated spectrum has been subtracted. The poor statistics in the neutron-gated spectrum is mainly due to the relatively low efficiency of the neutron detector, approximately 20% for a single neutron under the kinematic conditions of the present work.) Comparison of the two spectra clearly identifies those transitions which are in coincidence with neutrons. The four peaks marked with an "x" at the top of Fig. 2 correspond to transitions previously reported in ^{39}Cl from a study of the $(t, p\gamma)$ reaction [16]. Most of the remaining peaks in this spectrum, marked with a "c," can all be associated with reactions on trace chemical contaminants of the target; these reactions are predicted by the statistical model to be quite prolific. These contaminants include oxygen, present at a level of approximately 0.5 at. %, and silicon, at a considerably lower level. The latter is believed to result from cracking of ambient silicon-containing vapor arising from the use of silicone-based adhesive in assembling the phoswich telescopes. The relatively strong peak at 437 keV almost certainly comes from ^{42}Ca. Its presence in the $\alpha pn\gamma$ coincidence spectrum appears puzzling at first, since rejection of the $3n$ channel would be sufficient to preclude a peak of the strength observed. A likely possibility is that it results from $\alpha 2n$ evaporation on a ^{12}C contaminant in the target. This reaction is predicted by CASCADE to have a strong (60 mb) cross section. The 4π array could then attribute an αp signature to events where one of the two neutrons interacted in one of the plastic ΔE detectors, producing a recoil proton. Note that the relatively long lifetime of the 6^+ state in ^{42}Ca implies that delayed γ rays can simulate neutrons in the time-of-flight n-γ discrimination method used, thereby enhancing these lines relative to those of other possible contaminants.

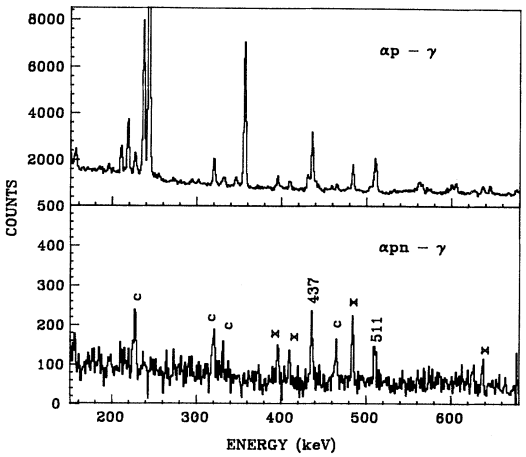

FIG. 2. The γ-ray spectrum in coincidence with one α particle, one proton, and a neutron (bottom) compared to the pure charged-particle (αp) gated spectrum (top). The spectrum shown is the sum of six Ge detectors. Known transitions in ^{39}Cl are marked with an "x"; the lines marked "c" are attributed to reactions on target contaminants.

B. Level scheme of ^{40}Cl

A two-dimensional matrix of all γ-γ events in coincidence with an α particle and a proton was constructed for analysis of the coincidence data. The statistics of the matrix were considerably improved by including α parti-

cles that were stopped in the thin plastic ΔE detectors, as suggested by the charged-particle E-ΔE spectra in coincidence with known γ transitions in ^{40}Cl. The final matrix contained a total of approximately 10^6 random subtracted α-p-γ-γ events. Sample coincidence spectra extracted from this matrix are shown in Figs. 3 and 4. The lower-energy part of the spectrum in coincidence with the 244 keV transition, the strongest transition in ^{40}Cl, is shown in Fig. 3(a). The four strongest transitions in this spectrum at 220, 238, 357, and 437 keV were previously identified by Kozub *et al.* [3]. Figure 3(b) shows the high-energy portion of the summed coincidence spectum gated on the 238, 244, and 357 keV γ rays. None of the transitions labeled in Fig. 3(b) were previously observed. As a second example, the existence of three γ rays at energies near 600 keV is demonstrated in Fig. 4; only the 601 keV line has been previously reported [3].

The experimental level scheme shown in the central portion of Fig. 5 has been constructed on the basis of the coincidence relationships of the observed transitions and their relative intensities, as shown in Table I. The suggested spins and parities were obtained from the angular distribution information inferred from the intensity ratios shown in Table I, from the (very limited) information on lifetimes obtained from the γ-ray line shapes, and from the usual assumption that fusion-evaporation reactions predominantly populate yrast and near-yrast states. The spin and parity suggestions for individual levels are discussed below.

The β^- decay of ^{40}Cl has previously been investigated (cf. Refs. [17], [18], and [19] and references therein) and the $\ln ft$ values measured for 38 levels in ^{40}Ar support $J^\pi = 2^-$ for the ground state of ^{40}Cl. Since the present reaction mechanism predominantly populates yrast states, the spin assignments for the states at 244, 601, and 839 keV follow directly from the angular distributions of the 244, 357, and 238 keV transitions which are consistent with $\Delta J = 1$. The angular distribution of the weak crossover 601 keV transition to the negative parity ground state is not measured with sufficient preci-

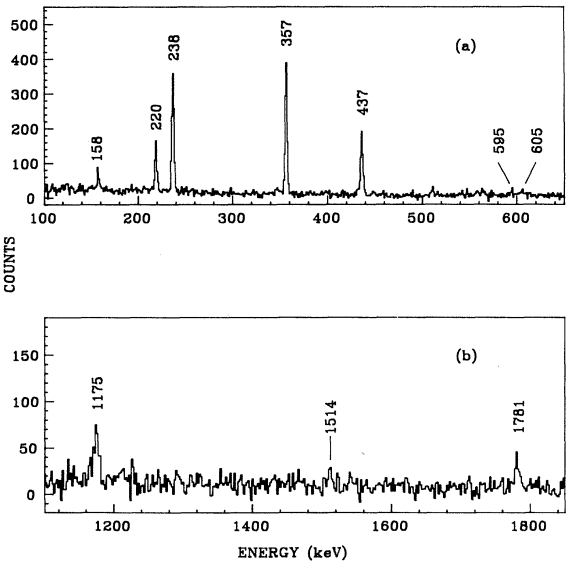

FIG. 3. (a) The spectrum in coincidence with the strongest transition in ^{40}Cl (244 keV), one α particle, and one proton; (b) high-energy part of the summed coincidence spectra gated on the 238, 244, and 357 keV transitions.

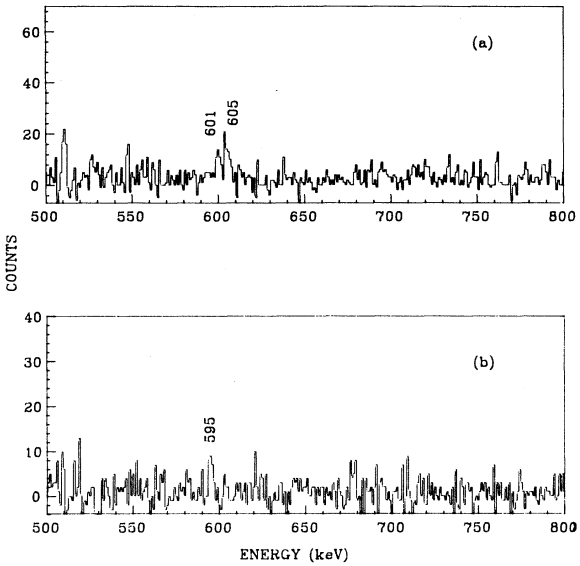

FIG. 4. Gated spectra illustrating the presence of three γ rays near $E_\gamma = 600$ keV: (a) sum of 1175 and 238 keV gates; (b) sum of 1175, 1781, and 605 keV gates.

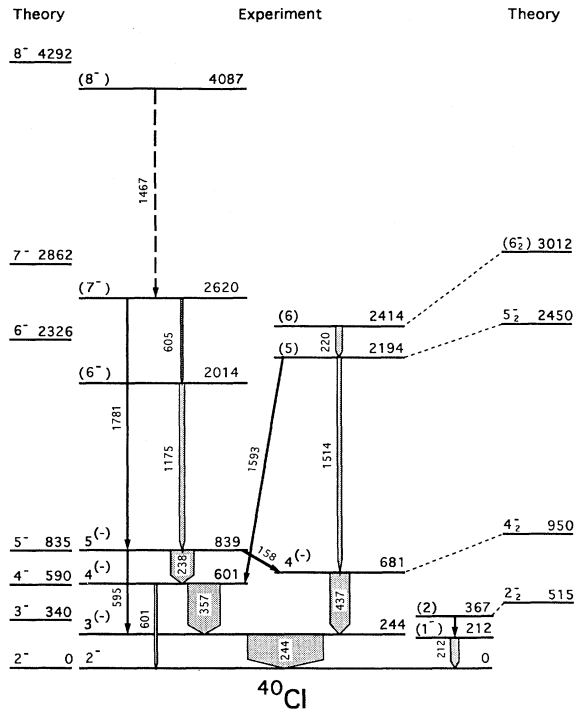

FIG. 5. The level scheme of ^{40}Cl deduced from the present work (center) compared to the predictions of [6]. The 155.5 keV transition (see Table I) connects the $E_x = 367$ and 212 keV levels; the 431.8 and 676.7 keV γ rays listed in Table I were associated with ^{40}Cl but not placed in the decay scheme.

TABLE I. Experimental γ-ray intensities and 135°/90° yield ratios.

E_γ	I_γ[a]	R (135°/90°)
155.5 (3)	0.4 (2)	b
157.8 (3)	3.0 (2)	0.84 (17)
211.7 (2)	11.0 (5)	0.99 (8)
219.6 (2)	9.0 (5)	0.67 (6)
237.9 (2)	31 (1)	0.83 (5)
244.0 (2)	100 (2)	0.96 (3)
357.5 (2)	43 (2)	0.94 (3)
431.8 (3)	10 (1)	0.99 (10)
437.0 (2)	26 (2)	0.87 (10)
594.9 (4)	2.3 (5)	b
600.9 (3)	3.7 (5)	b
605.4 (6)	3.3 (1.0)[c]	b
676.7 (3)	3.2 (5)	0.96 (30)
1175.4 (3)	7.1 (2.0)[c]	b
1466.7 (6)	1.0 (7)	b
1513.6 (4)	6.0 (2.0)	0.70 (30)
1592.5 (4)	2.5 (5)	b
1781.4 (5)	1.4 (5)	b
2075	< 0.6	b

[a]Efficiency corrected A_0, normalized to the 244 keV transition.

[b]Transition too weak to extract meaningful angular distribution.

[c]Intensity taken from spectrum at 90°.

sion to add much support to the $J = 4$ assignment of the 601 keV level. $E2$ multipolarity is suggested here, but a parity changing $M2$ cannot be ruled out by the data. The upper lifetime limit of 10 ns for the 601 keV state obtained from electronic timing yields a lower limit of $B(M2) \geq 0.38$ Weisskopf unit (W.u.) for the 8% branch which is well within the recommended upper limit. By the same argument the existence of the 595 keV crossover transition lends weak support to an assignment of $J = 5$ for the 839 keV level. An upper lifetime limit of 15 ns for the initial state of the 244 keV transition obtained from electronic timing does not provide a sufficient constraint to deduce the parity of the $J = 3$ state. However, it is strongly suggested that these levels belong to the $J^\pi = (2-5)^-$ multiplet obtained (in the simple weak-coupling picture) by coupling of the $J^\pi = 3/2^+$ ground state of ^{37}Cl to the $J^\pi = 7/2^-$ ground state of ^{43}Ca and therefore have negative parity.

All the states above 1 MeV were previously unobserved. For the levels at $E_x = 2014$ and 2620 keV, the existence of the 1781 keV crossover transition suggests a quadrupole in parallel with two $\Delta J = 1$ dipoles. Both the 1175 and 605 keV γ rays show strong Doppler shifts in the experiment utilizing the thick Be target, suggesting an apparent lifetime comparable to the stopping time of a few ps. While this does not rigorously rule out a strong $E2$ [a 1 W.u. $E2$ corresponds to a mean lifetime $\tau = 43$ ps at 1175 keV and 1.2 ns at 605 keV] it does in our view justify the suggestion that these are the 6^- and 7^- yrast states. The $E_x = 4087$ keV level is somewhat more uncertain than the others. The presence of an unresolved line which is present in the $\alpha pn\gamma$ coincidence spectrum (assumed to be a previously unknown transition in ^{39}Cl or from a reaction on a target contaminant) precludes either measurement of an angular distribution or any statement about the lifetime. The suggested spin and parity of 8^- should therefore be regarded as extremely tentative.

The $J = 4$ assignment of the 681 keV state is deduced from the fact that the 135°/90° yield ratios of both the 158 and the 437 keV γ rays are consistent with dipole transitions. A 681 keV crossover decay was not observed. In addition, the 437 keV transition shows clear evidence of a Doppler-shifted component, presumably from unobserved fast feeding. A 50 W.u. $E2$ corresponds to a lifetime of 123 ps, providing additional evidence in favor of dipole multipolarity for this line. (It is worth noting that there is a transition of nearly identical energy in the very prolific $3n$ reaction product ^{42}Ca. Its contribution to the $\alpha p\gamma$ and $\alpha p\gamma\gamma$ coincidence spectra of interest here is negligible.) The ordering of the 2194 and 2414 keV levels is suggested by the observation of the weak 1593 keV transition and is approximately consistent with the observed intensities, especially given the substantial uncertainties. Extraction of the angular distribution for the 1514 keV transition, as well as the possible existence of a Doppler-shifted component, is complicated by the presence of an unidentified line at approximately 1509 keV. Straightforward integration of the stopped component of the 1514 keV line suggest a ratio of counts at 135° and 90° which is considerably less than unity. Since the 220 keV line shows no evidence for a Doppler-shifted component, we believe that only a small part of the deficit at 135° for the 1514 keV line can be attributed to Doppler shifts, presumably from weak unobserved fast feeding of the 2194 keV level. This would suggest a mixed dipole-quadrupole character for the 1514 keV transition and, with the usual assumption concerning the population of near-yrast levels, imply a probable spin of 5. The spin of 6 suggested for the 2413 keV level follows from the dipole character of the 220 keV transition. The spins suggested for both of these levels are clearly tentative.

The 212 keV transition was the strongest transition previously observed in a study of the β decay of ^{40}S [2]. In the present data this transition was not observed in coincidence with the 244 keV γ ray or any other γ ray in coincidence with the latter, suggesting that it directly feeds the ground state. The $J^\pi = 1^-$ assignment for the 212 keV state was previously suggested by Warburton and Becker [6] based on a model-dependent argument. All three shell-model calculations predict the first excited state of ^{40}Cl to have $J^\pi = 1^-$ at an excitation energy ranging from 64 to 253 keV. A 155 keV transition was the only γ ray clearly identified in the spectrum in coincidence with the 212 keV line (and vice versa).

The level scheme shown in Fig. 5 does not include the 432 and 677 keV transitions listed in Table I and identified as transitions in ^{40}Cl. Both transitions were also observed in the study of the β decay of ^{40}S to ^{40}Cl by Dufour *et al.* [2]. The γ-ray spectra in coincidence with both transitions were inconclusive. In addition, a 347 keV γ ray was found to be in coincidence with the 244, 437, and 220 keV transitions but could not be placed in the decay scheme.

Upper limits on the lifetime for levels in ^{40}Cl were obtained from electronic timing. The fast response from the plastic scinitillators ($\tau \approx 2$ ns) used as ΔE detectors in the particle telescopes makes possible electronic timing down to a few ns. No delayed γ rays were observed; the upper lifetime limit inferred from the particle-γ timing spectra is about 15 ns at 200 keV and 3 ns at 1800 keV.

IV. DISCUSSION AND COMPARISON WITH THEORY

A summary of the experimental and theoretical information on excitation energies of negative parity states up to about 1 MeV in ^{40}Cl is given in Fig. 6. The first excited states were reported by Fifield *et al.* [1] using the charge exchange reaction ^{40}Ar(^{7}Li,^{7}Be) ^{40}Cl. The uncertainties in the energies of 30–40 keV due to the limited energy resolution of the particle detectors are indicated by the shaded areas in the first column.

All the states proposed by Kozub *et al.* [3] obtained from an in-beam γ-ray experiment using the ^{9}Be(^{36}S,αp)^{40}Cl reaction are shown in the second column of Fig. 6. Note that the level at 900 keV in this column is based on the 220 keV γ ray decaying to the 681 keV state. In the present work we have placed the 220 keV transition higher in the level scheme than was done in Ref. [3]. The 220 keV transition thus depopulates a level at $E_x = 2414$ keV. Two new γ rays with energies of 1514 and 1593 keV depopulate the 2194 keV level; these were not observed by Kozub *et al.*, who did not report any transitions with E_γ greater than 601 keV. The summed intensities of the two new transitions are approximately equal to that of the 220 keV transition (see Table I).

The results of the present work for the states below 1 MeV in column three are shown in comparison to the states predicted by the shell-model calculations of Warburton and Becker [6]. Note that a constant offset of 208 keV has to be added to the values published in Ref. [6] for all 3^- and 4^- states in order to obtain the correct excitation energies [20]. The corrected levels are shown in the fourth column. These shell-model results are in very good agreement with the experimental findings. The mean deviation of the excitation energies for the six excited states shown in Fig. 6 is 95 keV.

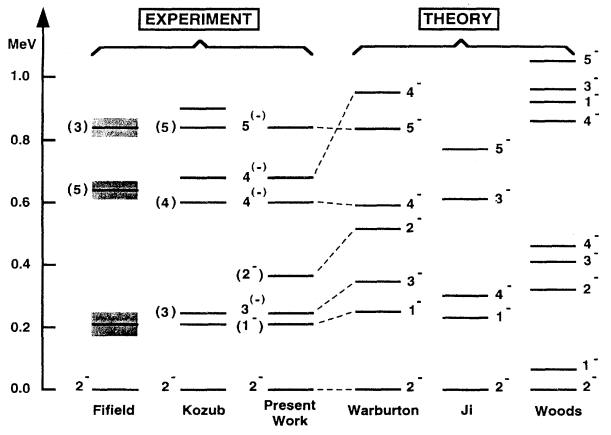

FIG. 6. Summary of the experimental and theoretical negative parity levels below 1 MeV excitation energy.

The predictions of Ji and Wildenthal [5] have been included in the fifth column of Fig. 6. This calculation was based on a shell-model space of valence neutron and proton $1d_{3/2}$, $1f_{7/2}$ orbitals where the parameters for an effective interaction between the valence particles were adjusted to reproduce the excitation energies of low-lying levels in this mass region. This leads to notably different results compared to other two calculations where the *sd* shell was fully (Warburton and Becker [6]) or partially (Woods [4]) included in the model space. In particular, the second excited state is predicted to have $J^\pi = 4^-$ and the first 3^- state lies about 300 keV higher, in contradiction with experiment. The rather poor agreement suggests that the $0d_{3/2}$-$0f_{7/2}$ model space is insufficient and that the effect of the $1s_{1/2}$ and $1p_{3/2}$ orbitals, which were not included in this calculation, is not negligible.

The calculation by Woods [4] using the Chung-Wildenthal matrix elements for the *sd* shell, shown in the last column of Fig. 6, produces all the states observed experimentally below about 1 MeV with a mean deviation of 149 keV. Woods' second calculation, using the Wildenthal "universal" *sd*-shell interaction, does not generate a second 4^- below about 1.5 MeV and was therefore not included in the present comparison.

In addition to the low-lying energy levels discussed above, the present work provides for the first time experimental information on higher-spin states with excitation energies above 1 MeV. These are states that, in a simple weak-coupling model, go beyond the coupling of the ground state of ^{37}Cl to the ground state of ^{43}Ca. Only the work of Ref. [6] reports predictions for states with $J > 5$. Experimental and theoretical excitation energies for the negative parity yrast states are compared in Fig. 5, with the theoretical predictions shown on the left. The theoretical results are in good agreement with experiment. The predictions are systematically somewhat too high with a mean deviation for the 6, 7, and 8^- yrast states of 252 keV.

Further insight concerning the success of the shell-model calculation of [6] can be obtained from a consideration of the information obtained regarding electromagnetic transition probabilities, both the experimental branching ratios and the limited information on level lifetimes. To begin with the negative parity yrast states, Warburton and Becker predict lifetimes of 23, 90, and 23 ps, respectively, for the lowest 3^-, 4^-, and 5^- levels. This is consistent with the observation of no Doppler-shifted components for the 244, 357, and 238 keV transitions. The experimental branching ratios for this $(2\text{-}5)^-$ multiplet are also well accounted for, the calculation predicting dominant $M1$ decays and weak $E2$ crossovers in agreement with experiment. The relative intensity of the 601 keV transition is experimentally observed to be about half the predicted value, whereas for the 5^- state the relative intensities of the 238, 595, and 158 keV transitions are all reproduced to better than 10%, assuming

the latter is identified with the transition to the second 4^- state. For the higher yrast states the calculation predicts shorter lifetimes (0.7 and 0.9 ps, respectively, for the yrast 6^- and 7^- states) in agreement with the observation of Doppler-shifted components for the 1175 and 606 keV transitions. The relative branching of the yrast 7^- state is also quite well reproduced by the calculation, which predicts nearly equal branches to the yrast 5^- and 6^- states, as observed. The very limited experimental information on the tentatively proposed (8^-) state is consistent with the calculation: a 25% $E2$ crossover is predicted, consistent with the upper limit of about 40% for the (unobserved) 2075 keV transition to the (6^-) state. Unfortunately, the present data do not permit a more quantitative asssessment of the absolute transition probabilities.

The comparison of the experimental branching ratios with theory for the nonyrast states beyond the 5_1^--4_2^- transition already noted is limited by the fact that we are unable to make a unique association between the calculated levels and those observed experimentally. For example, in the calculation of [6] there are 31 negative parity states below $E_x = 3$ MeV, whereas only 12 levels are observed in the present work. This is to be expected if the fusion-evaporation reaction mechanism strongly favors decays through yrast and near-yrast states. Possible theoretical counterparts for some of the nonyrast levels are shown on the right side of Fig. 5. The 5_2^- and 6_2^- levels are predicted at $E_x = 2450$ and 3012 MeV, respectively, and may be tentatively associated with the experimental levels at 2194 and 2413 keV. With this association, the dominant branch of the 5_2^- state to the 4_2^- state is correctly predicted; the substantial branch (approximately 30%) observed to the 4_1^- is negligible in the calculation. For the possible second 6^- state the situation is even worse. The theory predicts a strong decay to the lowest 5^- state, whereas experiment suggests only a decay to the (possible) second 5^- state. In a similar vein, the experimental level at 367 keV could be associated with the second 2^- state in the calculation. However, the model state decays predominantly to the ground state, whereas the 367 keV state decays only to the lowest 1^- state. Further speculation along these lines is not worthwhile until the experimental spins and parities are placed on a firmer foundation. In addition, it would be useful to have additional information concerning nonyrast levels which may have been missed in the present experiment.

Finally, it is interesting to note that attempts have been made to infer information about the ordering of the low-lying levels of ^{40}Cl by extrapolation from less neutron-rich systems. For example, Fifield *et al.* [1] suggested spin assignments for the low-lying 2^--5^- multiplet by analogy with ^{38}Cl. This would not be expected to work well. In the simplest shell-model picture, ^{38}Cl is described as $(\pi d_{3/2})^{-3} \times (\nu f_{7/2})^1$ whereas ^{40}Cl has two additional neutrons in the $f_{7/2}$ shell. The two additional neutrons can have a strong influence on the level ordering, as can be seen by comparing the level schemes of ^{40}K $[(\pi d_{3/2})^{-1}(\nu f_{7/2})^1]$ and ^{42}K $[(\pi d_{3/2})^{-1}(\nu f_{7/2})^3]$. A better semiempirical estimate of the ^{40}Cl level order can be obtained by treating the three $f_{7/2}$ neutrons as a single particle and applying a Pandya particle-hole transformation to the experimental level scheme of ^{42}K. This procedure predicts the 3^-, 4^-, and 5^- states at excitation energies of 344, 589, and 794 keV, in excellent agreement with experiment.

V. CONCLUSIONS

The present work establishes the yrast level scheme of ^{40}Cl up to a tentative spin $8\hbar$ and 4.087 MeV of excitation. A total of 18 γ transitions were identified and assigned to ^{40}Cl on the basis of charged-particle-γ and charged-particle-neutron-γ coincidences. The γ-γ coincidence relationships and relative γ-ray intensities lead to a level scheme of ^{40}Cl comprised of 16 transitions. Spins and (somewhat more tentatively) parities have been suggested for most of the levels observed. The experimental results are compared to theoretical predictions of three different shell-model calulations. Both the level energies and relative electromagnetic decays of the yrast negative parity states up to $J^\pi = (8^-)$ are well accounted for by a shell-model calculation utilizing the full *sdfp* model space. The results suggest that the shell-model can give a quantitative description of neutron-rich nuclei in this mass region.

The present work also demonstrates that the simultaneous detection of multiple charged particles in coincidence with γ rays (in the present case fourfold coincidences) is a very powerful tool for the investigation of very neutron-rich nuclei. We note that useful spectroscopic information has been obtained for transitions with intensities of approximately 1% of the strongest transition in a reaction channel which accounts for much less than 1% of the total reaction cross section. This corresponds to a level of sensitivity which is comparable to that achieved in the best work which has been done to date with recoil mass separators [21].

ACKNOWLEDGMENTS

We would like to acknowledge Dr. Roy Middleton and Harry White for assistance with the ^{36}S beam and Laszlo Csihas for making the high-purity Be targets. We are indebted to Lorenzo Farriss for assistance in performing the experiments. Two of the Ge detectors and a BGO Compton suppressor used in the present experimental work were kindly loaned to us by Professor J. Cizewski of Rutgers University. One of us (U.J.H.) would like to express his appreciation for stimulating communications with Dr. E. K. Warburton. We thank K. R. Pohl for considerable assistance with analysis of the data and for many valuable discussions. We are also indebted to Dr. D. F. Winchell for assistance with the calculation of Doppler-broadened line shapes. Financial support for this work was provided by the National Science Foundation.

[1] L. K. Fifield, M. A. C. Hotchtis, P. V. Drumm, T. R. Ophel, G. D. Putt, and D. C. Weisser, Nucl. Phys. **A417**, 534 (1984).
[2] J. P. Dufour, R. Del Moral, A. Fleury, F. Hubert, D. Jean, M. S. Pravikoff, H. Delagrange, H. Geissel, and K.-H. Schmidt, Z. Phys. A **324**, 487 (1986).
[3] R. L. Kozub, J. F. Shriner, Jr., M. M. Hindi, R. Holzmann, R. V. F. Janssens, T. L. Khoo, W. C. Ma, M. Drigert, U. Garg, and J. J. Kolata, Phys. Rev. C **37**, 1791 (1988).
[4] C. L. Woods, Nucl. Phys. **A451**, 413 (1986).
[5] X. Ji and B. H. Wildenthal, Phys. Rev. C **39**, 701 (1989).
[6] E. K. Warburton and J. A. Becker, Phys. Rev. C **39**, 1535 (1989).
[7] T. Chapuran, J. W. Arrison, D. P. Balamuth, and J. Görres, Nucl. Instrum. Methods A **272**, 767 (1988).
[8] R. Middleton, Nucl. Instrum. Methods **214**, 139 (1983).
[9] F. Pühlhofer, Nucl. Phys. **A280**, 267 (1977).
[10] A. Gavron, Phys. Rev. C **21**, 230 (1980).
[11] J. W. Arrison, D. P. Balamuth, T. Chapuran, D. G. Popescu, J. Görres, and U. J. Hüttmeier, Phys. Rev. C **40**, 2010 (1989).
[12] H. H. Eggenhuisen, L. P. Ekström, G. A. P. Engelbertink, and H. J. M. Aarts, Nucl. Phys. **A305**, 245 (1978).
[13] P. H. Kutt and D. P. Balamuth, Comp. Phys. **3**(5), 52 (1989).
[14] P. H. Kutt, data-acquisition and analysis program PLB (unpublished).
[15] See, for example, P. M. Endt, Nucl. Phys. **A521**, 1 (1990).
[16] E. K. Warburton, J. W. Olness, and G. A. P. Engelbertink, Phys. Rev. C **7**, 170 (1973).
[17] H. Morinaga, Phys. Rev. **103**, 504 (1956).
[18] G. Klotz, J. P. Gonidec, P. Baumann, and G. Walter, Nucl. Phys. **A197**, 229 (1972).
[19] P. M. Endt and C. van der Leun, Nucl. Phys. **A310**, 428 (1978).
[20] E. K. Warburton (private communication).
[21] C. J. Lister, A. A. Chishti, W. Gelletly, L. Goettig, R. Moscrop, B. J. Varley, A. N. James, T. Morrison, H. G. Price, J. Simpson, K. Connell, and O. Skeppstedt, Phys. Rev. Lett. **59**, 1270 (1987).

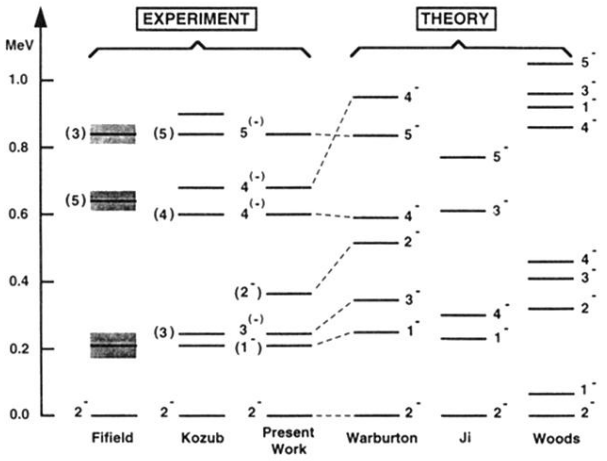

FIG. 6. Summary of the experimental and theoretical negative parity levels below 1 MeV excitation energy.